Pergamon

Int. J. Heat Mass Transfer. Vol. 39, No. 11, pp. 2293–2301, 1996

0017-9310/96 $15.00+0.00

0017–9310(95)00309–6

High temperature heat transfer of separated flow over a sudden-expansion with base mass injection

JING-TANG YANG and CHUN-HUNG TSAI

Department of Power Mechanical Engineering, National Tsing Hua University, Hsinchu, Taiwan 30043, Republic of China

(*Received* 15 *March* 1995 *and in final form* 14 *August* 1995)

Abstract—The high-temperature heat transfer characteristics of the hot flow stream over a sudden-expansion with cold air uniformly injected from a porous base was investigated. The heat transfer coefficient increased with increasing inlet temperature and Reynolds number, but decreased with increasing injection rate of the cooling air. The local Nusselt number was affected by the Reynolds number at the inlet in the whole flow field except near the step ($X/H < 4$). The local Stanton number, however, was insensitive to the Reynolds number in the recirculation zone. After the recirculation zone, the local Stanton number was affected by the Reynolds number, although to a lesser extent than that of the Nusselt number. Copyright © 1996 Elsevier Science Ltd.

INTRODUCTION

The air stream over a sudden-expansion produces a separated flow containing a recirculating flow, a shear layer and a re-developing boundary layer. Such a flow pattern is related to various devices such as diffusers, airfoils and combustors. In combustion systems, the sudden-expansion is a typical component which is used for flame holding because it is stable, easy to control, and causes large variations of the flow patterns and local heat transfer coefficient over a simple geometry. In such a combustor, the flame is held at the step and the shear layer above the solid fuel surface. The fuel surface was heated by the flame and the fuel vapour pyrolysis into the flame zone to enhance combustion. The heat transfer behaviors and the flow characteristics of the combustor are complicated because of the interaction of the blowing effect from the fuel surface and the main flow. Much attention was attracted to this type of problem.

Many previous investigations over a backward-facing step had been conducted, extensive efforts were devoted to the features of cold flow, such as the reattachment length and turbulent flow structures without mass injection [1]. Furthermore, a number of studies on a combustor were carried out on the overall efficiency of combustion or flame structure such as Schadow *et al.* [2], Zvuloni *et al.* [3]. To elucidate the detailed phenomena and mechanism of ignition and combustion, the analysis of the heat transfer characteristics is needed.

Most previous researchers regarded heat transfer with a cold inlet flow over the sudden-expansion with the base at either a constant temperature [4, 5] or a constant heat flux [6–9]. Aung [4] used a Mach–Zehnder interferometer to investigate the temperature distribution of the laminar flow behind a backward-facing step with constant wall temperature, and pointed out that the heat transfer coefficient increased monotonously downstream. Tsou *et al.* [5] showed the transient behavior of the heat transfer characteristics. Filetti and Kays [8] reported that both the maximum heat transfer coefficient and the Nusselt number were located at the reattachment point. Sparrow *et al.* [6] and Vogel and Eaton [7] discovered that the maximum Nusselt number was located upstream of the reattachment point. Zvuloni *et al.* [3] reported that the highest heat transfer coefficient appeared near the reattachment point in their investigation of reacting flow over a backward-facing step. Baek *et al.* [10] investigated the buoyancy-assisting flow in a vertical backstep and reported that higher temperature difference reduced the reattachment length and increased the Nusselt number.

Previous investigations mostly treated the phenomena of cold flow with a hot boundary and with the temperature difference normally less than 30°C. The heat transfer behavior with a great temperature difference between the flow and the wall was rarely studied. In addition, in a combustor the flow is hot which heated the cool wall, and the situation is opposite to the conventional cooling analysis. Cheng *et al.* [11] investigated laminar flow heat transfer in a rectangular duct with one-walled injection and constant heat flux. They found that the heat transfer was decreased in injection conditions. Soong and Hsueh [12] studied the heat transfer behavior in a separated flow field at constant wall conditions with a slit cold injection gas, for which the temperature difference between the wall and inlet flow was about 30°C. For the higher temperature flow situation, Yogesh and Raghunandan [13] investigated flame structure and

NOMENCLATURE

H	step height
h	heat transfer coefficient
k	thermal conductivity
Re	Reynolds number
St	Stanton number
Nu	Nusselt number
q''	local heat flux to the wall
Q	injection flow rate
T	mean temperature
$T.I.$	turbulent intensity
U	horizontal velocity
V	vertical velocity
X	horizontal distance from the step
X_r	reattachment length
Y	vertical distance from the base wall.

Greek symbols

ρ	density of air
ϕ	the porosity of the porous plate.

Subscripts

f	working fluid
s	porous plate
max	maximum value
o	inlet condition
w	injected property
wall	porous wall condition.

the characteristics of heat transfer of inlet gas temperature 120°C in a reacting flow and injected fuel from the base wall. Their experiments reported that the heat transfer was decreased with gas injection and increased at higher inlet velocity. The wall heat transfer behaviors in a combustion condition are similar to those without flame. However, their experiments were limited to a small velocity (1.5 m s^{-1}) in a narrow range ($X/H < 5$) shorter than the recirculation zone and provided no detailed data of how the pyrolyzed fuel vapor affected the fluid dynamics and heat transfer behavior. Yang and Tsai [14] developed the experimental apparatus to explore the heat transfer behavior of the high temperature flow and reported some experimental data. But the physical insights need to be systematically investigated.

In this present work we investigate the heat transfer characteristics in a combustor with inlet flow velocity up to 40 m s^{-1} and flow temperature up to 400°C and the temperature difference between the main flow and the base is up to 200°C. The cold air was injected uniformly into the test section through its base and was controlled at a fixed temperature of 25°C, which is to simulate the case of either pyrolysis of fuel vapor or the film cooling by the cold fluid.

EXPERIMENTAL DESIGN

Test rig and instrumentation

The experiments were conducted in an open-circuit wind tunnel that supplied a hot flow stream under specified conditions. A schematic diagram of the wind tunnel and instrumentation is shown in Fig. 1. The air flow was supplied by a 75-kW Roots blower with speed controlled by a frequency inverter (HITACHI). The flow stream entering the test section was high-temperature gas (200–400°C), which consisted of the combustion products of liquefied petroleum gas (LPG) and air generated in a vitiator before the settling chamber. As the overall ratio of air to fuel in the experiment was greater than 100, the combustion products only took less than 1% of the air flow rate, therefore, the properties of the fluid entering the test section were almost identical to air.

The cross-section of the combustor entrance was 30 mm high and 200 mm wide. The aspect ratio (channel width to step height) for the step height (15 mm) was 13.3. The base of the test section was a steel porous plate with pore diameter 100 μm, which allowed cold air to be injected uniformly into the test section. Thermocouples (K-type, 125 μm, coated with a thin film of polymer for insulation) were adhered to both sides of the porous plate for heat flux measurement on the base wall, as shown in Fig. 2. The injected air was supplied by a compressor (11 kW) and monitored by a rotameter. The injected air temperature was maintained at a constant level on the outer wall of the base, the same as Yogesh and Raghunandan [13]. To maintain a fixed boundary condition, the temperature of the injected air was kept at 25°C by a small heat exchanger which was installed beneath the porous plate.

The inlet velocity was measured with a two-component (four-beam) forward-scattering laser-Doppler velocimeter (LDV, TSI). The inlet temperature was measured with a K-type thermocouple and a digital thermometer (FLUKE 2190A). The temperature in the flow field was measured with a K-type thermocouple wire which was wrapped by a thin ceramic tube and a 2.5-mm-diameter L-shaped stainless steel tube, which was inserted into the flow field from the edge of the test section subtending 45° to the horizontal direction to minimize interference. The measurement probe was moved by a two-dimensional traverse table.

Test conditions and data accuracy

The inlet velocity varied from 10.5 to 44.9 m s^{-1} and the corresponding Reynolds number, based on the step height, varied from 3130 to 12 900. The injec-

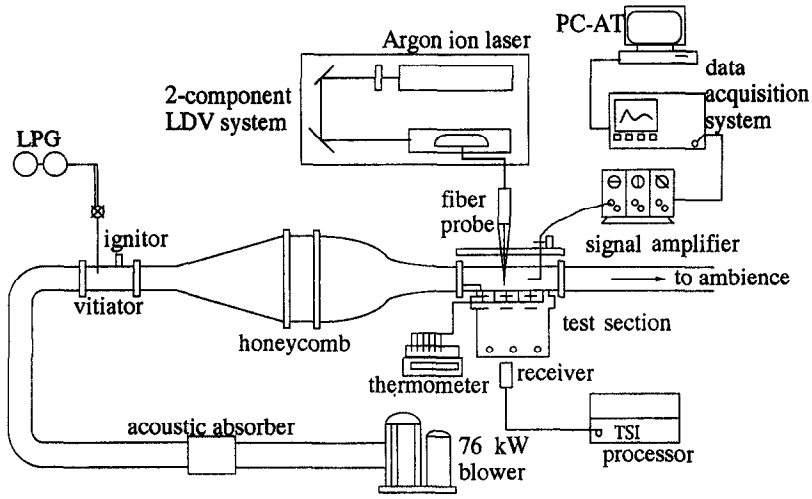

Fig. 1. Schematic diagram of experimental apparatus.

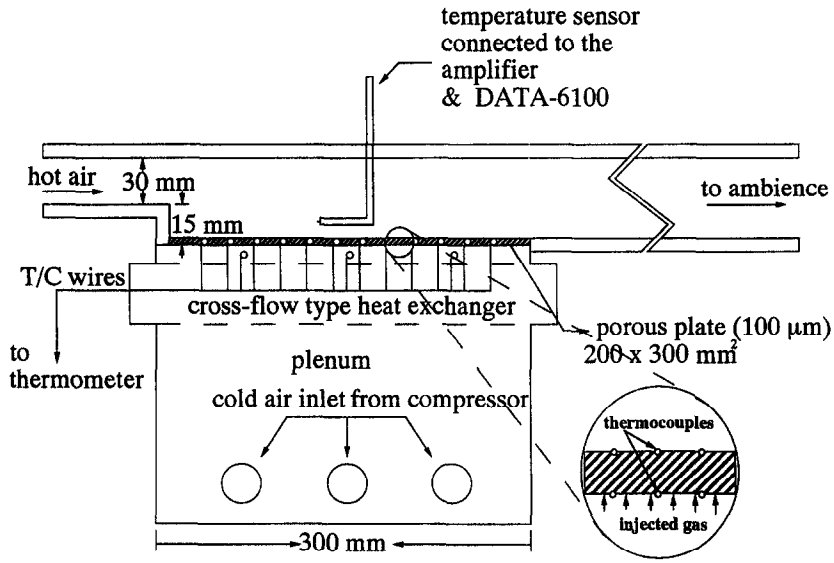

Fig. 2. Configuration and dimensions of the test section.

tion rate through the base wall ranged from 0 to 350 l/min, which produced the superficial injection flow velocity 0–0.17 m s^{-1}. The inlet temperatures of the flow were 25, 200, 300 and 400°C. The heat transfer and flow structure were studied quantitatively through measurements of the temperature across the porous plate, velocity and velocity fluctuations in the flow field within the combustor.

The entry flow conditions corresponding to all the tests are summarized in Table 1. The boundary layer thicknesses, based on 99% of the free stream velocity, were varied in the range 7–9 mm, the momentum thicknesses were 0.41–0.89 mm, and the thermal boundary layer thicknesses were 8 9 mm. The Reynolds number based on the step height, UH/ν ranged between 3130 and 12900. The shape factors (displacement thickness to momentum thickness) were 1.1–1.2. According to Pitz and Daily [15], the shape factor of Blasius flow is about 2.4 and that of fully turbulent flow is about 1.3. The boundary layer is in a transitional region for Re_θ from 250 to 1800 [1] and the reattachment length is not independent of Reynolds number (or in the fully turbulent regime) until Re_θ is about 1800. The Reynolds number based on the momentum thickness in this work ranged between 160 and 388. Also the reattachment length varied from 6 to 8 step heights. All the data indicate that the experimental conditions were located in the transitional region from laminar to turbulent flow.

As the aspect ratio of the test section exceeds 10, the flow field is regarded as two-dimensional [16]. The temperature distributions in the spanwise direction of the porous plate were uniform over 80% of the test section, thus the heat transfer in the spanwise direction was neglected in this investigation. The uncertainty of the wall temperature measurements was within 1.5%.

Table 1. Entry conditions of the experiments

Inlet temperature and velocity	Reynolds number, UH/ν	Boundary layer thickness (mm)	Momentum thickness θ (mm)	Shape factor, H_{12}	Momentum Reynolds number, $U\theta/\nu$	T.I./U_0 (%) Free stream	T.I./U_0 (%) Boundary layer	Thermal boundary layer thickness (mm)
200°C and 15–30 m s^{-1}	6250–12 900	7–8	0.41–0.49	1.10–1.12	235–253	3.3–5.0	6.7–9.1	—
300°C and 10–35 m s^{-1}	3130–11 000	7–8	0.50–0.89	1.16–1.17	160–313	3.6–5.6	7.4–9.0	8–9
400°C and 25–40 m s^{-1}	6000–9370	9	0.74–0.79	1.17–1.20	198–388	7.1–7.2	10.0–11.9	—

The radiation heat transfer between the flow and the wall was neglected because it was less than 1% of overall heat transfer rate. The 95% confidence level of the mean temperature data was less than 2.0%. The heat transfer coefficient and the Nusselt number was within 3.0%. During collection of the inlet velocity data, 2048 typical measurements were made. The 95% confidence levels of the mean velocity and the turbulence intensity were 4.3% and 4.9%, respectively.

RESULTS AND DISCUSSION

Length of the recirculation zone

The length of the recirculation zone of varied temperatures and Reynolds numbers are shown in Fig. 3. For the temperature of the inlet flow of 400°C, the length approached 7.8 times the step height when the Reynolds number exceeded 6300. The length of the recirculation zone (reattachment length) was in the same range compared to previous works [4, 5, 12]. Varied inlet temperatures cause different viscosities which change the Reynolds number of the flow, even though the inlet velocities remain constant. For high temperature flows, the length of the recirculation zone increased rapidly with the Reynolds number until it exceeded 7000; after that it increased slightly with increasing Reynolds number. As the mass injection rate remained invariable, the inlet gas with a higher temperature generated a longer recirculation zone. The length of the recirculation zone in the cold flow was much less than that in hot flow conditions, and it approached a constant at a greater Reynolds number compared with the hot flow. The effects of the mass injection on the size of the recirculation zone are shown in Fig. 4. In the cold flow tests, the length of the recirculation zone decreased with increasing rate of the injection gas, which was consistent with Richardson *et al.* [17]. For example, the length of the recirculation zone at injection velocity 0.17 m s^{-1} was 10% less than that without injection. The effects of the injection gas on the length of the recirculation zone in high temperature flow conditions were similar to that of the cold flow. However, the reduction of the length with injection gas was more profound at a smaller Reynolds number because the flow momentum in the near wall region was smaller, thus the influence of the injected gas became more significant. As the Reynolds number exceeded 8600 in the hot

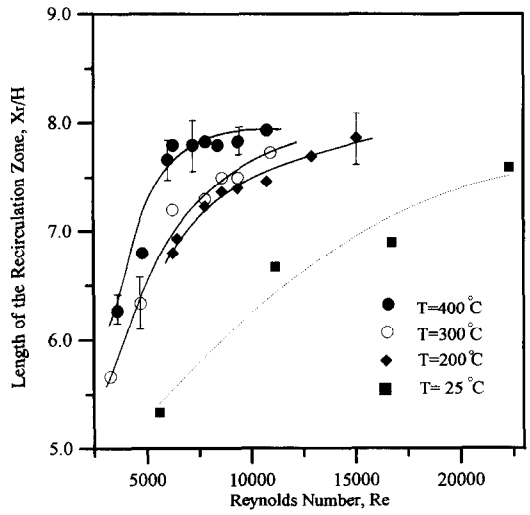

Fig. 3. Variations of the length of the recirculation zone with Reynolds number at various flow temperatures; Q = 250 l min^{-1}, T_0 = 25, 200, 300 and 400°C.

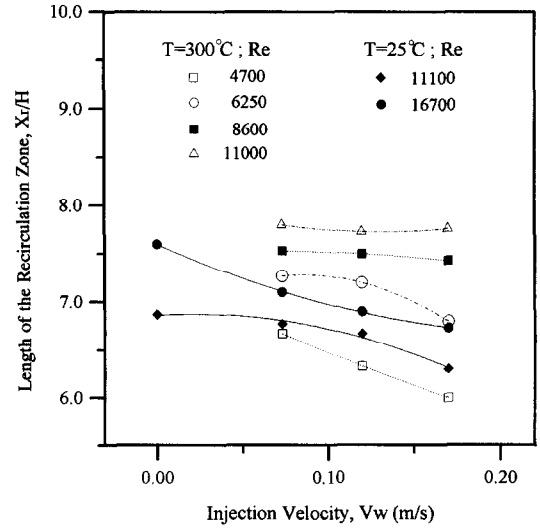

Fig. 4. Variations of the length of the recirculation zone with injection flow rates at various Reynolds number and temperatures; T_0 = 25, 300°C, Q = 0, 150, 250, 350 l min^{-1}.

flow, the injected mass only slightly affected the size of the recirculation zone.

Temperature profile

The profiles of temperature distribution in horizontal positions for an inlet fluid temperature of 300°C at three different injection flow rates are shown in Fig. 5. The distributions differ from other cold flow data [4, 7] because the directions of the heat transfer are opposites. The temperature profiles of the free stream above the recirculation zone were nearly the same as that of the upstream profile in the inlet, when the inlet temperature and velocity of the flow were 300°C, 25 m s^{-1} and the base wall injected gas was 250 l min^{-1}. The temperatures in the recirculation zone were much lower than those of the free stream, since only less than one sixth of the high temperature gas in the shear layer entered the recirculation zone [18]. As the flow velocity was relatively small in the recirculation zone the heat transfer was dominated by conduction, whereas the flow outside the recirculation zone was dominated by convective mixing. Two significant temperature gradients appeared in the temperature profiles; one in the shear layer and the other near the wall. In the shear layer the temperature gradient was the largest because of the strongest turbulent mixing between the free stream and the recirculating flow. The large temperature gradient adjacent to the wall

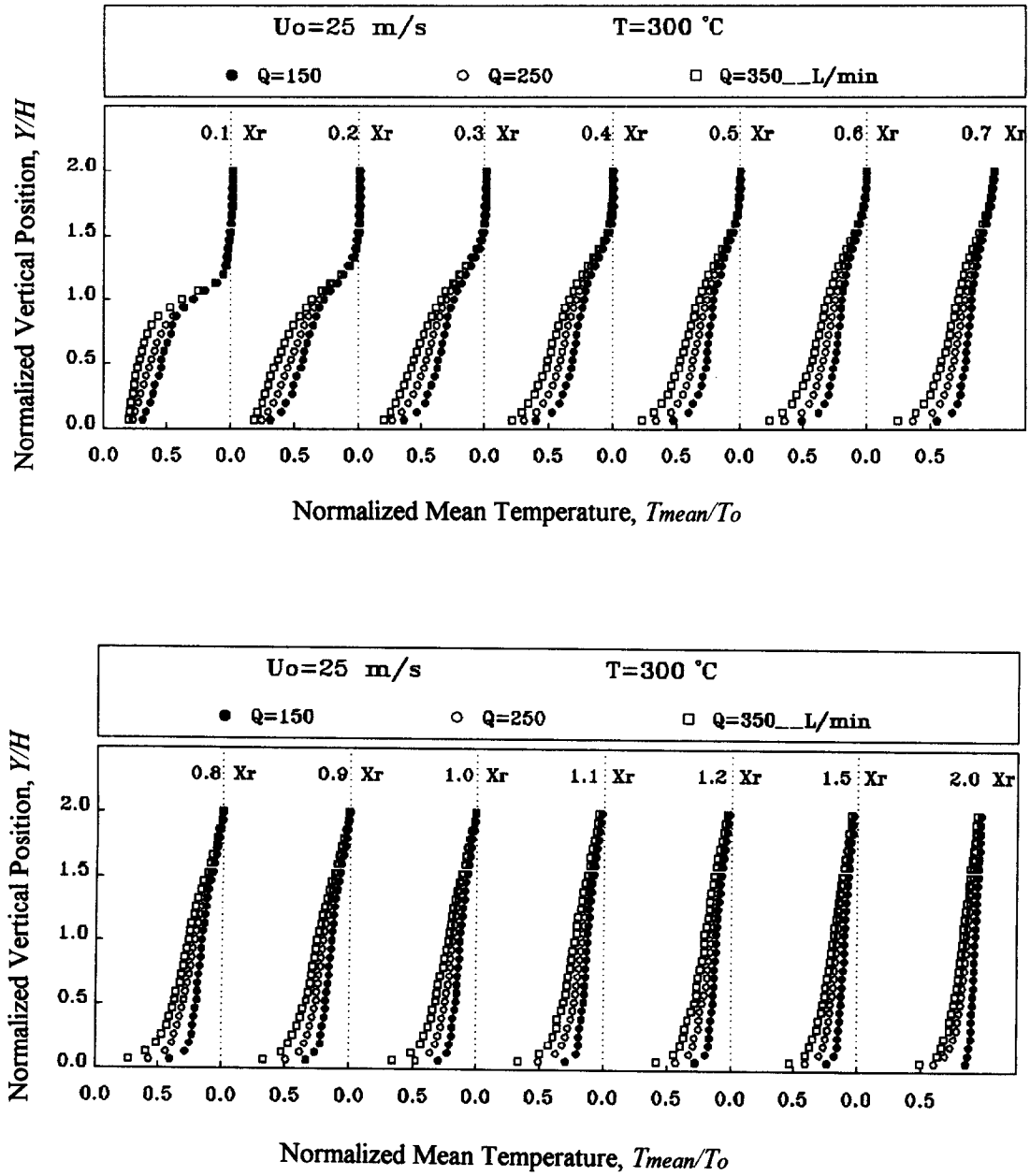

Fig. 5. Variations of normalized temperature profiles in horizontal direction at various injection flow rates; T = 300°C, U_o = 25 m s^{-1}, Q = 150, 250 and 350 l min^{-1}.

showed a strong cooling effect owing to the injected cool flow. The temperature gradient near the step, 0.1 X_r, was much lower than other locations because the bulk flow was nearly stagnant in the front part of the recirculation zone and was not well mixed with the high-temperature fluid. After the recirculation zone, the temperature profiles at varied locations were almost coincident, which indicated that the temperature field of the flow was well developed.

Variations of the temperature profiles at varied mass injection rates, shown in Fig. 5, indicate that the cooling effects of the injected fluid were more substantial in the recirculation zone than in other regions because the velocity in that region was much lower than in the free stream and the redeveloped boundary layer. In the cross-sections near the step ($X/X_r = 0.1, 0.2$), the injected fluid affected only the flow temperature below the step. As the bulk flow within the recirculation zone began to interact with the free stream in the shear layer around 0.3–0.4 X_r [19], the distinctions among the temperature profiles above the step height at three mass injection rates became apparent. The ranges that were affected by the injected cold fluid gradually extended into the free stream along the horizontal direction. After the recirculation zone the temperature distribution in the whole flow field was affected by the injection.

Local heat flux

The rate of heat transfer on the base wall is estimated based on the temperatures on both sides of the porous plate. The heat flux between the flow and the wall, q'', is calculated according to the following equations:

$$q'' = \rho_f C_{pf} V_w \Delta T + K_{eff} \frac{\Delta T}{\Delta Y} + K_{eff} \frac{\Delta T}{\Delta X} \quad (1)$$

$$K_{eff} = \phi k_f + (1-\phi) k_s, \quad (2)$$

where ΔT is the temperature difference on the both sides of the porous plate, ΔY is the thickness of the porous plate, ΔX is the horizontal distance, V_w is the injection velocity, ϕ is the porosity of the porous plate, k_f is the conductivity of the injection gas and k_s is the conductivity of the porous plate.

The first term of the right hand side of equation (1) is the heat flux absorbed by the injected fluid passing through the porous plate. It was the term used for estimating the wall heat flux by Yogesh and Raghunandan [13] and their data were of the same order as this study. The second term of the right hand side of equation (1) is the heat conduction in the vertical direction through the porous plate. It became larger at a greater inlet temperature and higher inlet velocity, but decreased with the increasing injection rate of the cooling flow. The third term of the right hand side of equation (1) is the heat conduction along the horizontal direction through the porous plate. The amounts of heat flux contributed by the three different terms for heat transfer on the porous plate are shown in Fig. 6. The conduction heat transfer in the vertical direction on the porous plate dominates the total heat flux because of the great effective conductivity and the other contents are less than 4% of the total heat flux. Because the injected cold fluid mixed with the hot flow fluid near the porous plate and decreased the mean temperature in the boundary layer above the porous plate, the heat transfer rate from the hot flow to the plate was thus decreased.

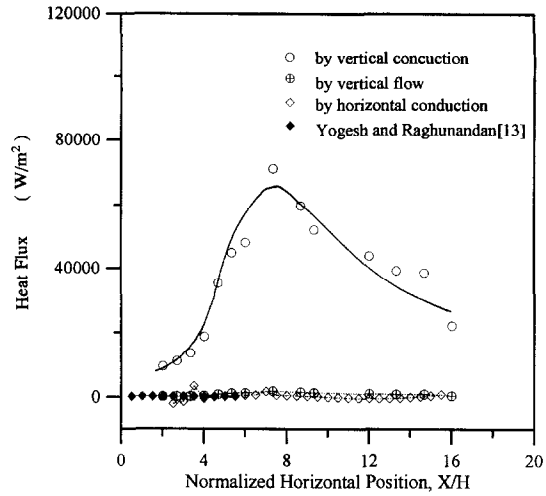

Fig. 6. Various types of heat flux to surface in horizontal direction; $U_o = 20$ m s^{-1}, $T_o = 300$°C, $Q = 250$ l min^{-1}.

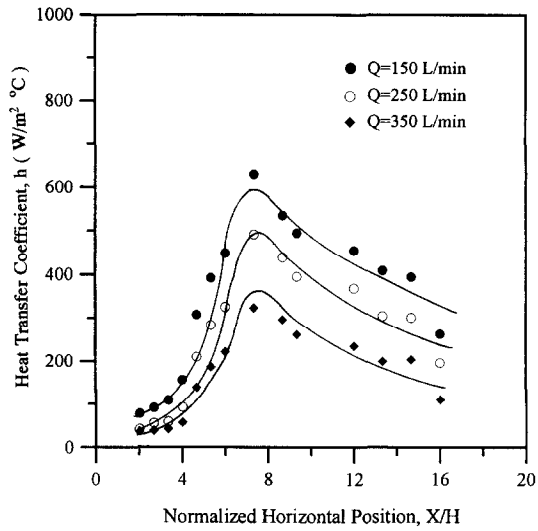

Fig. 7. Variations of heat transfer coefficient in horizontal direction at various injection flow rates; $U_o = 25$ m s^{-1}, $T_o = 200$°C, $Q = 150$, 250 and 350 l min^{-1}.

Effects of mass injection on heat transfer

The heat transfer coefficient was calculated by the following equation:

$$h = \frac{q''}{T_o - T_{wall}}. \quad (3)$$

Figure 7 shows that the local heat transfer coefficient

increased along the streamwise direction in the recirculation zone, reached a maximum value near the mean reattachment, then decreased gradually downstream. The result was similar to the previous work of Sparrow *et al.* [6] and Vogel and Eaton [7]. Since the injected cold flow from the wall of the porous base reduced the mean temperature in the boundary layer on the base wall (Fig. 5), the wall heat transfer, and thus the local heat transfer coefficient, decreased with increasing injection rate. As a result, both the dimensionless heat transfer coefficient and the Nusselt number decreased.

Effects of Reynolds number on Nusselt and Stanton numbers

The Nusselt number and Stanton number are defined as follows:

$$Nu = \frac{hH}{k} \tag{4}$$

$$St = \frac{h}{\rho C_p u_\infty} = \frac{Nu}{RePr}. \tag{5}$$

The Nusselt number represents a dimensionless heat transfer coefficient and behaves similarly to the heat transfer coefficient. Figure 8 shows the dependence of the Nusselt number on the Reynolds number (based on the inlet velocity) at a fixed injection rate 250 l min^{-1} and various inlet flow temperatures. In the front portion of the recirculation zone ($X/H < 4$), the Nusselt numbers of all the inlet conditions were approximately constant because the corner of the recirculation zone was hardly affected by the variations of the free stream. Downstream of the position $X/H = 4$, the effects of the flow velocity and Reynolds number became profound. When the inlet velocity was fixed at 25 m s^{-1}, the Reynolds numbers of the inlet temperature 200, 300 and 400°C were 10750, 7800 and 6000. The flow of the same velocity with lower inlet temperature, thus a higher Reynolds number, enhances the Nusselt number on the wall. On the other hand, the flow at a higher temperature needs a greater velocity to keep the inlet Reynolds number the same. At a constant Reynolds number of 9370, the smaller temperature of the inlet flow enhanced the heat transfer in the recirculation zone, but decreased the heat transfer after recirculation zone. This might be caused by the turbulence intensity near the wall region and the reverse mass flow rate in the recirculation zone. Comparing the inlet conditions at a constant velocity and a constant Reynolds number, the effect of the Reynolds number on the Nusselt number are more significant than the inlet velocity. Similar to the trend of the heat transfer coefficient, a maximum Nusselt number was located around the end of the recirculation zone, and then decreased downstream. The effects of the Reynolds number and temperature on the Nusselt number were more profound after the recirculation zone.

The heat transfer behavior was further analyzed by the distributions of the Stanton number, which represents the ratio of actual heat flux from the fluid to the wall to the heat capacity of the fluid flow. The distributions of the Stanton number along the horizontal distance were plotted in Fig. 9, in which the inlet conditions were the same as those in Fig. 8. Because the ratio of the heat transfer to the heat capacity at the same Reynolds number of the inlet conditions was close, the effects of velocity were circumvented, and the curves of the three inlet temperatures corresponding to the same Reynolds number thus converged. In the situation with a constant inlet velocity but different temperature, the depen-

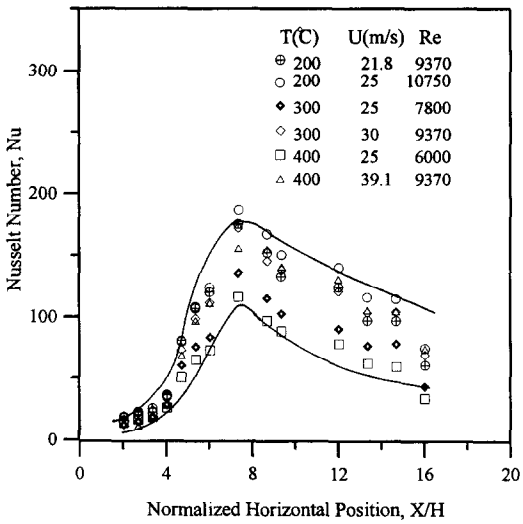

Fig. 8. Variations of Nusselt number in horizontal direction at various temperatures, Reynolds number and velocities; U_o = 21.8–39.1 m s^{-1}, T_o = 200, 300 and 400°C, Q = 250 l min^{-1}.

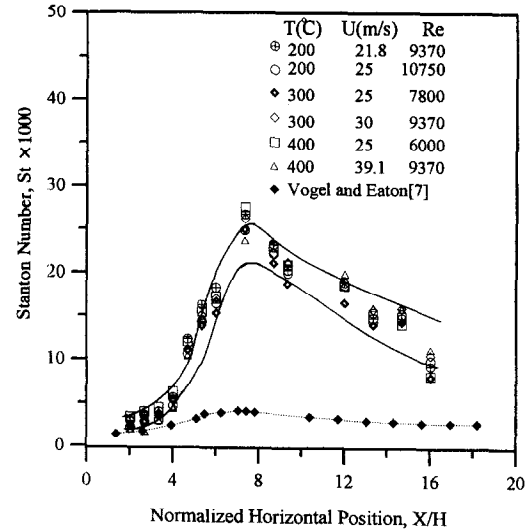

Fig. 9. Variations of Stanton number in horizontal direction at various temperatures. Reynolds number and velocities; U_o = 21.8–39.1 m s^{-1}, T = 200, 300 and 400°C, Q = 250 l min^{-1}.

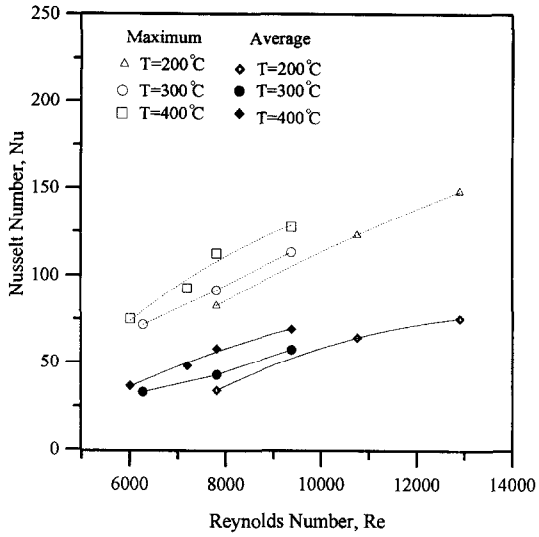

Fig. 10. Variations of maximum and average Nusselt number in Reynolds number at various temperatures. T_0 = 200, 300, 400°C, Q = 350 l min^{-1}.

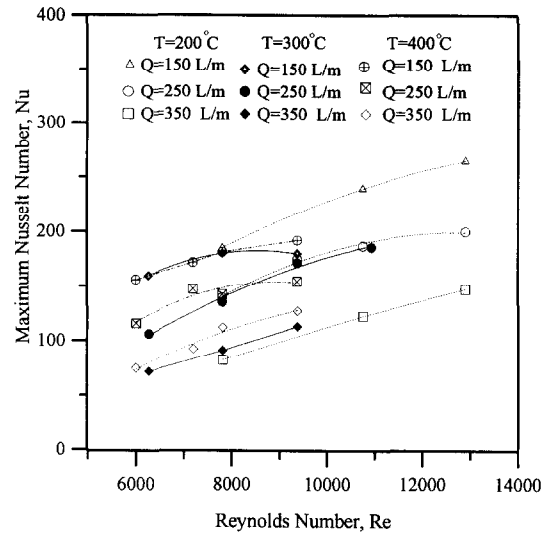

Fig. 11. Variations of maximum Nusselt number in Reynolds number at various temperatures and injection flow rates; T_0 = 200, 300 and 400°C, Q = 150, 250 and 300 l min^{-1}.

dence of the Stanton number on flow temperature or Reynolds number downstream of the recirculation zone was relatively significant. It was similar to that of Nusselt number in Fig. 8, although the variations were less distinct. The Reynolds number must have caused certain alterations other than changing the heat capacity on the flow structure and the wall heat transfer after the recirculation zone, otherwise the four curves should have converged too.

Variations of the maximum and average Nusselt number in the horizontal direction, at various Reynolds numbers, are shown in Fig. 10. The gas was injected at 350 l min^{-1} and the temperatures of the inlet were 200, 300 and 400°C, respectively. The tendency of the maximum and average Nusselt number on varied Reynolds number was similar, but the maximum values were approximately two times the average values. Variations of the maximum Nusselt number and Stanton number with the Reynolds number at various temperatures and injection rates are plotted in Figs. 11 and 12. Both the maximum Nusselt number and Stanton number occurred at the end of the recirculation zone. At a fixed Reynolds number, the maximum Nusselt number decreased in a higher rate of injected gas as well as that of the maximum Stanton number. At the largest gas injection 350 l min^{-1}, the higher temperature enlarged the maximum Nusselt number as well as that of the Stanton number. When the injected gas was 150 l min^{-1}, the lower temperature enlarged the maximum Nusselt number and the maximum Stanton number. All the maximum Nusselt numbers increased with raising Reynolds number because that carried more heat into the test section. But the maximum Stanton numbers were nearly the same or decreased with the higher Reynolds number. This indicates that in higher Reynolds number, the amounts of heat flux entering the base

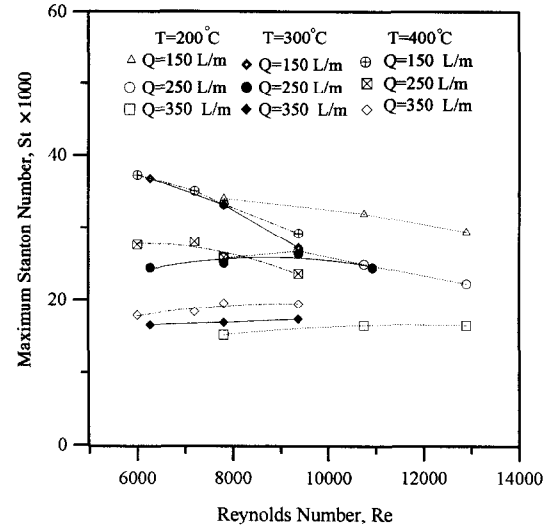

Fig. 12. Variations of maximum Stanton number in Reynolds number at various temperatures and injection flow rates; T_0 = 200, 300 and 400°C, Q = 150, 250 and 300 l min^{-1}.

surface are less than the heat capacity carried by the main stream. The heat capacity is exhausted out of the test section. This result is consistent with that of Vogel and Eaton [7].

CONCLUSIONS

In this work we successfully developed the experiment to investigate the high-temperature heat transfer of a hot flow stream flowing over a sudden-expansion with cold air injected from its porous base. The results show that the Reynolds number and inlet temperature are the major influential factors on the size of the recirculation zone, the heat transfer coefficient

and Nusselt number. A greater inlet temperature and Reynolds number extended the recirculation zone, whereas the increased injection rate shortened the length.

The temperatures in the recirculation zone are much lower than those of the free stream, since only less than one sixth of the high temperature shear layer flow enters the recirculation zone. The cooling effects of the injected fluid were more substantial in the recirculation zone than other regions because the velocity in that region was much smaller than in the free stream and the redeveloped boundary layer. After the recirculation zone, the temperature profiles at varied locations are almost coincident, which indicated that the temperature field of the flow had been well developed.

The wall heat transfer was contributed by heat conduction in both vertical and horizontal directions and the convective heat absorbed by the injected fluid, and the vertical conduction accounted for over 96% of the total heat transfer. The heat transfer coefficient increased with increasing inlet temperature and Reynolds number, but decreased with the increasing injection rate of the cooling air. In addition, the maximum heat transfer coefficient was located near the end of the recirculation zone.

The Nusselt number was affected by the Reynolds number at the inlet in the whole flow field except near the step ($X/H < 4$). The heat transfer coefficient normalized by the heat capacity (Stanton number) was insensitive to the Reynolds number in the recirculation zone. After the recirculation zone, the Stanton number was still affected by the Reynolds number, although to a lesser extent than that of the Nusselt number. The maximum and average Nusselt numbers were larger in a higher Reynolds number, but the values of the maximum and average Stanton number, however, remained unaffected or decreased in a greater Reynolds number. The results of this paper provide valuable information on the high-temperature heat transfer and fluid behavior of the hot flow over a sudden-expansion, and could be beneficial for the design of the combustor and for verification of the existing numerical models.

Acknowledgement—This work was financially supported by the National Science Council of the Republic of China under the contract no. CS82-0210-D-007-013 and Tsing Hua Fellowship. The authors wish to thank H. M. Law for building up the vitiator for the experiment.

REFERENCES

1. J. K. Eaton and J. P. Johnston, A review of research on subsonic turbulent flow reattachment, *AIAA J.* **19,** 1093–1100 (1981).
2. K. C. Schadow, H. F. Cordes and D. J. Chieze, Experiment studies of combustion process in a tabular combustor with fuel adding along the wall, *Combust. Sci. Technol.* **19,** 839–841 (1978).
3. R. Zvuloni, Y. Levy and A. Gany, Investigation of a small solid fuel ramjet combustor, *J. Propulsion Power* **5,** 269–275 (1989).
4. W. Aung, An experimental study of laminar heat transfer downstream of backsteps, *J. Heat Transfer* **105,** 823–829 (1983).
5. F. K. Tsou, S. J. Chen and W. Aung, Starting flow and heat transfer downstream of a backward-facing step, *J. Heat Transfer* **113,** 583–589 (1991).
6. E. M. Sparrow, S. S. Kang and W. Chuck, Relation between points of flow reattachment and maximum heat transfer for regions of flow separation, *Int. J. Heat Mass Transfer* **30,** 1237–1246 (1987).
7. J. C. Vogel and J. K. Eaton, Combined heat transfer and fluid dynamic measurements downstream of a backward-facing step, *J. Heat Transfer* **107,** 922–929 (1985).
8. E. G. Filetti and W. M. Kays, Heat transfer in separated, reattached, and redevelopment regions behind a double step at enterence to a flat duct, *J. Heat Transfer* **88,** 131–136 (1967).
9. N. Seki, S. Fukusako and T. Hirate, Turbulent fluctuations and heat transfer for separated flow associated with a double step at entrance to an enlarged flat duct, *J. Heat Transfer* **98,** 588–593 (1976).
10. B. J. Baek, B. F. Armaly and T. S. Chen, Measurements in buoyancy-assisting separated flow behind a vertical backward-facing step, *J. Heat Transfer* **115,** 403–408 (1993).
11. Y. C. Cheng, G. J. Hwang and M. L. Ng, Developing laminar flow and heat transfer in a rectangular duct with one-walled injection and suction, *Int. J. Heat Mass Transfer* **37,** 2601–2613 (1994).
12. C. Y Soong and W. C. Hsueh, Mixed convection in a suddenly-expanded channel with effects of cold fluid injection, *Int. J. Heat Mass Transfer* **36,** 1477–1484 (1993).
13. G. P. Yogesh and B. N. Raghunandan, Flow structure and heat transfer characteristics behind a diaphragm in the presence of a diffusion flame, *Int. J. Heat Mass Transfer* **32,** 19–28 (1989).
14. J. T. Yang and C. H. Tsai, Heat transfer of hot flow in a sudden-expansion combustor with vertical injection, *Proceedings the 8th International Symposium on Transport Phenomena in Combustion*, San Francisco, 16–20, July (1995).
15. R. W. Pitz and W. Daily, Combustion in a turbulent mixing layer formed at a rearward-facing step, *AIAA J.* **21,** 1565–1570 (1983).
16. V. de Brederode and P. Bradshaw, Three-dimensional flow in normal two-dimensional separation bubbles: I. flow behind a rearward-facing step, Aeronaut Report, 72-19, Imperial College, August (1972).
17. J. Richardson, W. A. de Groot, J. I. Jagoda, R. E. Waiterick, J. E. Hubbartt and E. C. Strahle, Solid fuel ramjet simulators results: experimental and analysis in cold flow, *J. Propulsion Power* **24,** 1956–1963 (1985).
18. D. W. Etheridge and P. H. Kemp, Measurement of turbulent flow downstream of a rearward-facing step, *J. Fluid Mech.* **86,** 545–566 (1978).
19. J. T. Yang, B. B. Tsai, and G. L. Tsai, Separated-reattaching flow over a backstep with uniform normal mass bleed, *J. Fluids Engng* **116,** 29–35 (1994).